International Journal of Pharmaceutics, 72 (1991) 65–77
© 1991 Elsevier Science Publishers B.V. 0378-5173/91/$03.50
ADONIS 037851739100208R

IJP 02406

Rheological study of w/o/w emulsion by a cone-and-plate viscometer: Negative thixotropy and shear-induced phase inversion

Yoshiaki Kawashimà, Tomoaki Hino, Hirofumi Takeuchi, Toshiyuki Niwa and Katsuhiko Horibe

Gifu Pharmaceutical University, 5-6-1 Mitahora-higashi, Gifu 502 (Japan)

(Received 25 June 1990)
(Modified version received 13 November 1990)
(Accepted 30 January 1991)

Key words: w/o/w emulsion; Cone-and-plate viscometer; Negative thixotropy; Semi-solidification; Phase inversion; Impulse application

Summary

The rheological behaviour of a w/o/w emulsion was examined by a cone-and-plate viscometer. Negative thixotropic flow patterns were observed at lower shear rates. This negative thixotropic behavior was more pronounced and the apparent viscosity increased under increased shear rate, prolonged shearing time, or repeated shear. Further shearing, by raising the shear rate or prolonging the shearing time, rapidly increased the shear stress of the emulsion and induced phase inversion. This phase-inverted emulsion was of the w/o type and in a semi-solid state. The energy dissipated by the flow of the emulsion until the occurrence of phase inversion, the kinetic energy of the emulsion at the phase-inversion point, and the impulse applied to the emulsion by the cone of the viscometer were calculated in order to determine the hydrodynamic parameter determining the phase inversion. The impulse applied by the rotating cone was the parameter determining the phase inversion of the emulsion from a w/o/w to a w/o type characterized by being in the semi-solid state. The negative thixotropic flow and the phase inversion of the w/o/w emulsion to the w/o type induced by shearing were explained as being due to the increase in the volume fraction of the oil droplets by entrapment of water molecules and by coalescence of the oil droplets.

Introduction

Water-in-oil-in-water multiple emulsions (w/o/w emulsions) have many potential applications to cosmetics (Lin et al., 1975), foods (Takahashi, 1986), and medical uses (Yoshioka, 1982; Fukushima, 1983). Quantitative investigations of the rheological properties of w/o/w emulsions on application are required in order to guarantee stability during storage and against the shear applied by handling or transportation.

In the present study, the stability of w/o/w emulsions against shear stress was precisely investigated by using a cone-and-plate viscometer. Plastic or negative thixotropic flow patterns were observed under lower shear. It was found that the

Correspondence: Y. Kawashima, Gifu Pharmaceutical University, 5-6-1 Mitahora-higashi, Gifu 502, Japan.

emulsion became semi-solid and that the phase inverted to a w/o type on shearing at a higher rate or when the shearing time was longer than a critical value.

The aim of this study was to analyze quantitatively the flow curves of w/o/w emulsions and the mechanism of shear-induced phase inversion by calculating the hydrodynamic parameters, i.e., dissipated energy, kinetic energy and impulse, applied to the emulsion by the rotating cone.

Materials and Methods

Materials

The lipophilic surfactant, sorbitan monooleate (Span 80), and hydrophilic surfactant, polyoxyethylene sorbitan monolaurate (Tween 20) (Kishida Chemical Co., Japan), were used without further purification. The liquid paraffin specified in the Japanese official formulary of food additives was used. All other chemicals used were reagent grade.

Preparation of w/o/w emulsion

w/o/w emulsion was prepared by the two-step emulsification procedure described by Matsumoto et al. (1976). 100 ml of 0.02 mol/l sodium chloride aqueous solution were added drop wise to 60 ml oil phase at a rate of 1.7–2.0 ml/min with the aid of a pump, CV-1 (Tokyo Kagakuseiki Co., Japan). The oil phase consisted of 70% w/v liquid paraffin and 30% w/w Span 80 (1st emulsification stage). During this stage, the system was agitated at 390 rpm by a Chemy Stirrer B-150 (Tokyo Rikakikai Co., Japan) with double four-bladed propellers. The resultant w/o emulsion was added to 160 ml of 0.5% w/v Tween 20 aqueous solution at a rate of 6.0–8.0 ml/min using the pump and agitated with the stirrer at 630 rpm (2nd emulsification stage).

In the second emulsifying step at 630 rpm with prolonged shearing time (> 30 min), phase inversion induced by the cone-and-plate viscometer was not observed, since the shear force brought about with the propellers only applied locally to the emulsion. The resultant w/o/w emulsion was stable during storage at 5 °C for 1 week after preparation.

Scanning electron microscographs of the freeze-fractured w/o/w emulsion were taken on a T330A (JEOL Ltd, Japan).

Percentages of w/o/w emulsion formed

10 ml w/o/w emulsion were placed in a seamless cellulose tube (Viskase Sales Corp., U.S.A.) and were dialyzed for 24 h in 90 ml of 0.5% w/v Tween 20 aqueous solutions.

The concentration of sodium chloride dialyzed in the medium was determined by electroconductivity measurements with a DS-7M (Horiba Co., Japan).

The percentages of w/o/w emulsion formed, α (%), were calculated according to Eqn 1:

$$n_{10}V_1(1 - \alpha/100) = n_1\left[V_d + V_s\{V_1(1 - \alpha/100) + V_2\}/(V_1 + V_2 + V_0)\right] \times (V_1 + V_2 + V_0)/V_s \quad (1)$$

where n_{10} denotes the initial concentration of sodium chloride in inner aqueous phase, n_1 is the concentration of sodium chloride dialyzed in the medium, V_1, V_2, V_0 represent the volumes of the inner aqueous phase, outer aqueous phase and oil phase in the formulation to prepare w/o/w emulsion, respectively, and V_d, V_s denote the volumes of dialysis medium and dialyzed emulsion, respectively.

If V^* is defined by Eqn 2, α is described by Eqn 3:

$$V^* = V_2 + V_d(V_1 + V_2 + V_0)/V_s \quad (2)$$

$$\alpha = 100\{1 - n_1V^*/(n_{10} - n_1)V_1\}. \quad (3)$$

Sodium chloride detected in the dialysis medium was assumed to originate only from the rupture of oil membrane during the dialysis and preparation of w/o/w emulsions. In this report, the permeation of water and sodium chloride through the oil membrane caused by an osmotic gradient was taken to be negligible, although it has been reported that water as well as the markers initially

added in the inner aqueous phase could migrate through oil membranes (Matsumoto, 1980; Garti, 1985; Magdassi, 1986; Ohmotosho, 1986).

A w/o/w emulsion containing 0.05 mol/l sodium chloride in the inner aqueous phase and 0.02 mol/l glucose and 0.05% w/v Tween 20 in the outer phase during preparation was also examined in order to investigate the intermixing of aqueous phases. This emulsion was dialyzed under the same conditions as described above. Glucose was detected spectrophotometrically at 490 nm by means of the phenol-sulfuric acid reaction (Dubois, 1956). The percentages of sodium chloride trapped in the inner aqueous phase (P_{NaCl}) and that of glucose ($P_{glucose}$) were calculated by using Eqns 8 and 9, respectively, introduced as follows.

$$n_{10}H_1 = n_1(V^* + H_1 - H_2) \tag{4}$$

$$n_{20}(V_2 - H_2) = n_2(V^* + H_1 - H_2) \tag{5}$$

where n_{20} is the initial concentration of glucose in the outer aqueous phase, n_2 denotes the detected concentration of glucose in the dialysis medium, H_1 is the volume of water expelled from the inner aqueous phase to the outer aqueous phase on rupture of the oil membrane and H_2 corresponds to the volume of water forced from the outer aqueous phase to the inner aqueous phase.

H_1 and H_2 are expressed by Eqns 6 and 7, respectively.

$$H_1 = n_1 n_{20}(V^* - V_2)/(n_{10}n_{20} - n_{10}n_2 - n_1 n_{20}) \tag{6}$$

$$H_2 = \{(n_{10} - n_1)n_{20}V_2 - n_{10}n_2V^*\} /(n_{10}n_{20} - n_{10}n_2 - n_1n_{20}) \tag{7}$$

$$P_{NaCl} = 100(V_1 - H_1)/V_1 \tag{8}$$

$$P_{glucose} = 100\ H_2/V_2 \tag{9}$$

Observation of flow behavior and its analysis

Rheological examination was carried out immediately after the preparation of w/o/w emulsions.

The cone-and-plate viscometer employed was a Rheometer NRM-O (Nippon Rheology KiKi Co., Japan). Cone radius and angle were 4.64 cm and 20′, respectively.

The w/o/w emulsion was sheared by rotating the cone, uniformly accelerated and decelerated, to observe rheological behavior at 20 °C. The program time, t_p, is the time required to reach the maximum speed of rotation of the cone. Shear rate, $\dot{\gamma}$ (s^{-1}) was calculated via Eqn 10:

$$\dot{\gamma} = \omega/\Theta \tag{10}$$

where ω is the angular velocity of the cone and Θ denotes the angle of the cone.

Casson plots (Casson, 1959) and log-log plots of shear stress vs shear rate were constructed in the analysis of flow curves of the w/o/w emulsion. Casson expressed shear stress of the dispersion system, σ, by means of Eqn 11:

$$\sigma^{1/2} = k_0 + k_1\dot{\gamma}^{1/2} \tag{11}$$

where k_0 is the shear stress at $\dot{\gamma} = 0$ and k_1 represents the square root of viscosity extrapolated to $\dot{\gamma} \to \infty$.

The regression lines of Casson plots, i.e., $\sigma^{1/2}$ vs $\dot{\gamma}^{1/2}$ were drawn by the least-squares method.

Log-log plots were constructed according to:

$$\sigma = k\dot{\gamma}^a \tag{12}$$

$$\ln \sigma = a \ln \dot{\gamma} + \ln k \tag{13}$$

where a and k are constants.

Results

The flow behavior of w/o/w emulsion under low shear

The percentage of w/o/w emulsion produced was found to be 86.4%. Fig. 1 shows an electron micrograph of a w/o/w emulsion produced in the present system.

The emulsion droplets had a diameter of 8–90 μm and contained many small aqueous droplets dispersed within them. Flow curves of the w/o/w

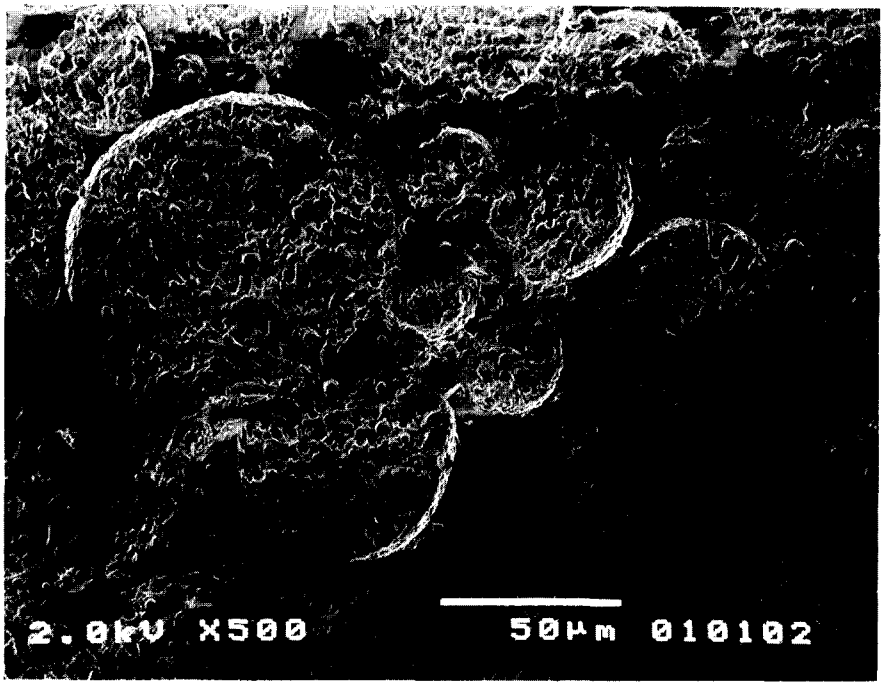

Fig. 1. Scanning electron micrograph of w/o/w emulsion.

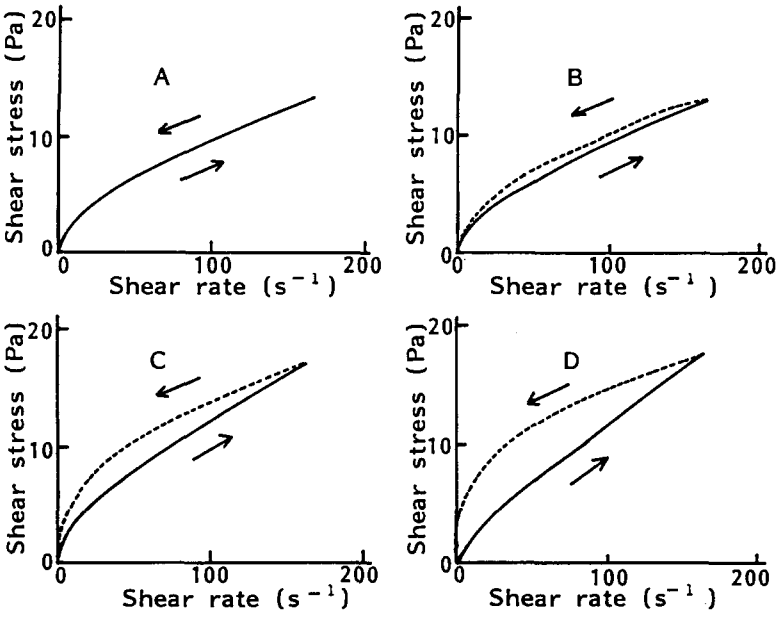

Fig. 2. Changes in flow curves on acceleration of shear rate. Maximum shear rate: 160 s^{-1}. Program time: (A) 60 s, (B) 300 s, (C) 600 s, (D) 900 s.

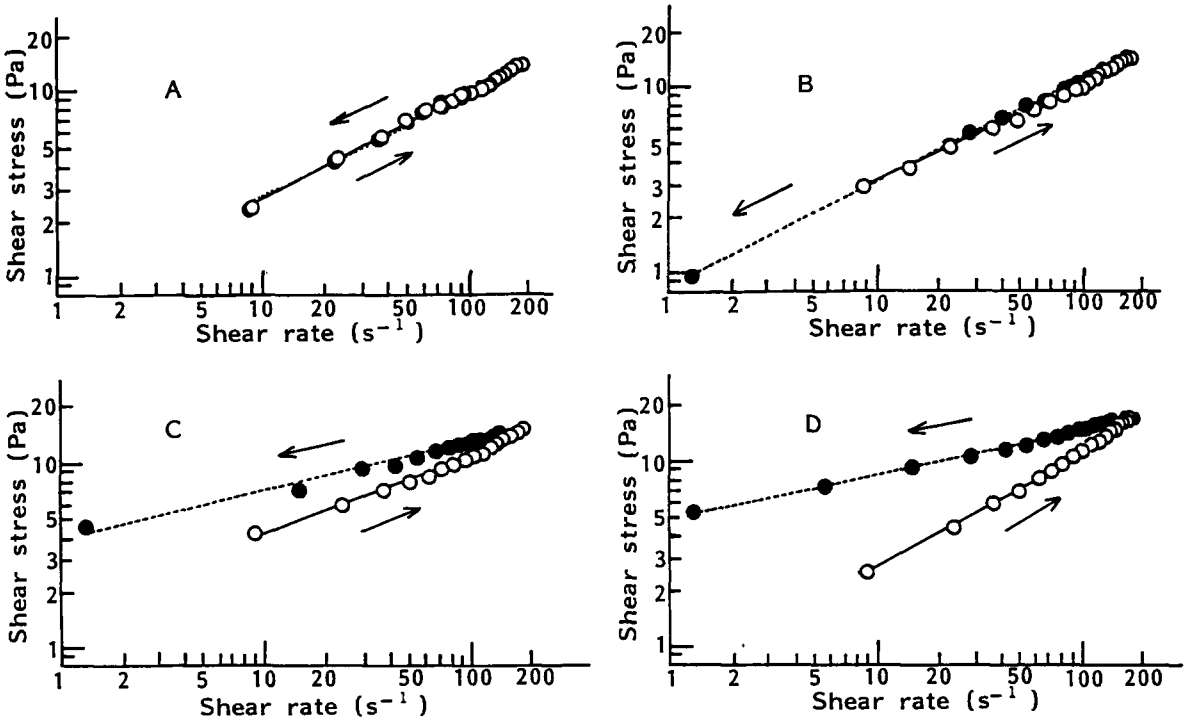

Fig. 3. Flow curves replotted on log-log scale. Maximum shear rate: 160 s^{-1}. Program time: (A) 60 s, (B) 300 s, (C) 600 s, (D) 900 s.

emulsion were obtained under various shear conditions.

Effects of acceleration of shear Flow curves observed under accelerated rotation of the cone and at its maximum shear rate (160 s^{-1}) are shown in Fig. 2.

All ascending and descending curves in Fig. 2 show negative thixotropic flow patterns characterized by two upper convex curves, whose descending portion shows more shear stress than that of the ascending portion. Both curves followed the same path when the program time was 60 s. With increasing program time, the negative thixotropy and the area of the hysteresis loop of the flow curves increased.

Casson plots and log-log plots of σ, $\dot{\gamma}$ were applied to analyze these flow curves. The regression of both Casson and log-log plots proved to be

TABLE 1

Parameters in Eqn 13 and loop areas of flow curves affected as a function of shear acceleration

Maximum shear rate (s^{-1})	Program time (s)	Ascending curve			Descending curve			Loop area (Pa s^{-1})
		a	*k*	*r* [a]	*a*	*k*	*r* [a]	
160	60	0.579	0.662	0.9981	0.594	0.614	0.9985	53.3
160	300	0.578	0.659	0.9946	0.563	0.745	0.9993	123.3
160	600	0.572	0.859	0.9935	0.411	2.050	0.9974	335.3
160	900	0.706	0.441	0.9943	0.382	2.530	0.9987	603.9

[a] *r*: correlation coefficient.

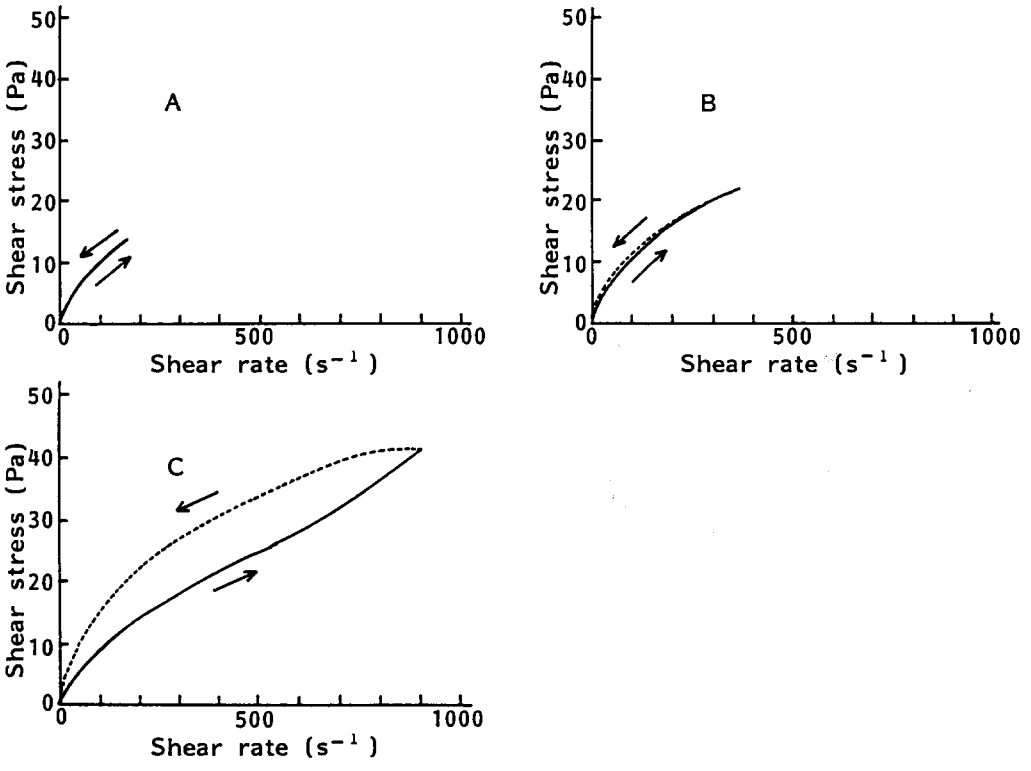

Fig. 4. Changes in hysteresis loop with shear rate. Maximum shear rate: (A) 180 s^{-1}, (B) 360 s^{-1}, (C) 900 s^{-1}. Program time: (A) 60 s, (B) 120 s, (C) 300 s.

correlated linearly with correlation coefficients > 0.994. Although Casson plots are widely employed to describe the rheological behavior of dispersion systems, the assumption that k_1 is constant is inappropriate because the Casson equation was derived under the assumption that the dispersion medium is a Newtonian liquid of constant viscosity. The modified Casson equation, the MTMO equation (Matsumoto, 1970), applicable for non-Newtonian flow systems is expressed by Eqn 14:

$$\sigma^{1/2} = k_0 + k_1(\eta_a/\eta_0)^{1/2}\dot{\gamma}^{1/2} \quad (14)$$

where η_0 and η_a are the zero-shear and apparent viscosity of the dispersion medium, respectively. The determination of apparent viscosities is difficult due to the migration of emulsifier molecules in the dispersion medium and through the oil membrane. Therefore, log-log plots are employed to analyze the flow curves in this study as shown in Fig. 3. The parameters, a and k, obtained from regression analyses of plots and the loop area are listed in Table 1.

Although the parameters a and k of the ascending curves did not correlate with the acceleration of cone rotation, a and k of the descending portions decreased and increased with increasing program time, respectively. The loop area increased with prolongation of program time as shown in Table 1.

These findings indicated that the sheared emulsion showed a negative thixotropic property and an increase in viscosity.

Effects of maximum shear rate on flow behavior

Fig. 4 shows the changes in flow curves with changing maximum shear rate. The acceleration of shear was fixed at 3 s^{-2}.

The ascending and descending flow curves coincided with each other at low maximum shear rate ($\leqq 360$ s^{-1}). A large hysteresis loop was observed at high maximum shear rate. The hysteresis loop appeared at higher maximum shear rates,

and the area of the loop increased with increase in maximum rate.

Effect of repeating time of shear on flow behavior The changes in flow curves on repeating the shear applied to the w/o/w emulsion are shown in Fig. 5. Maximum shear rate and program time were fixed at 900 s^{-1} and 120 s, respectively. The hysteresis loop area increased with repeated shearing emulsion.

Effects of holding time at maximum shear rate on flow curves The rotation of the cone was accelerated uniformly and held at a maximum shear rate of 900 s^{-1} for (A) 60, (B) 120 and (C) 180 s, respectively. It was then decelerated uniformly. The flow curves are shown in Fig. 6. Program time was fixed at 120 s.

Shear stress and loop area increased as the holding time at maximum shear rate was prolonged. The parameters, a and k, of the regression lines of the flow curves replotted on a log-log scale and the loop areas in Figs 4–6 are shown in Table 2.

Parameter a decreased, and parameter k increased, with increasing maximum shear rate applied to the emulsion, which indicated that the negative thixotropic property and the viscosity increased. The repeated shearing decreased in a of descending curves and increased in k of ascending and descending curves, indicating an increase in viscosity and negative thixotropy. Increases in shear stress and viscosity were found on prolonging the holding time at maximum shear rate, which

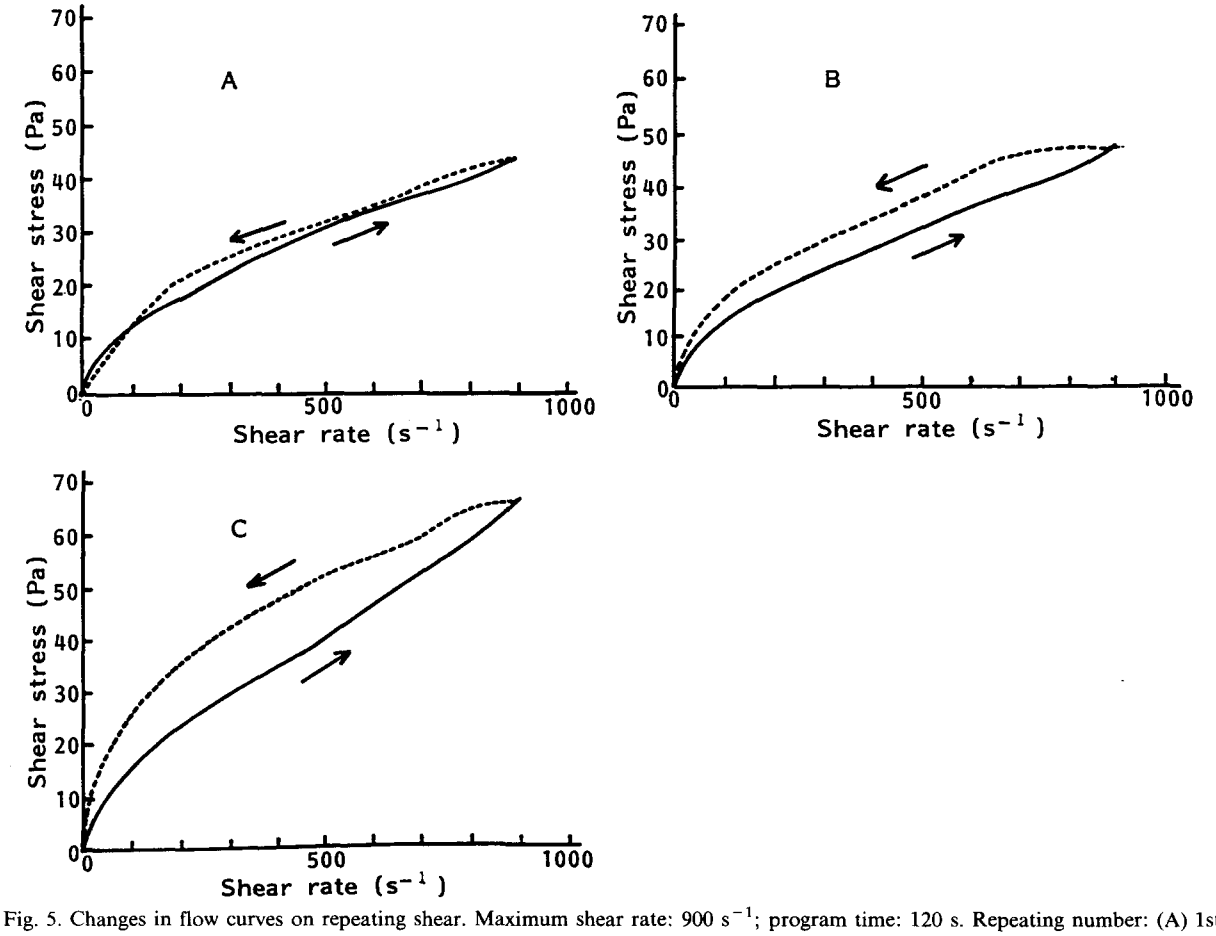

Fig. 5. Changes in flow curves on repeating shear. Maximum shear rate: 900 s^{-1}; program time: 120 s. Repeating number: (A) 1st run, (B) 2nd run, (C) 3rd run.

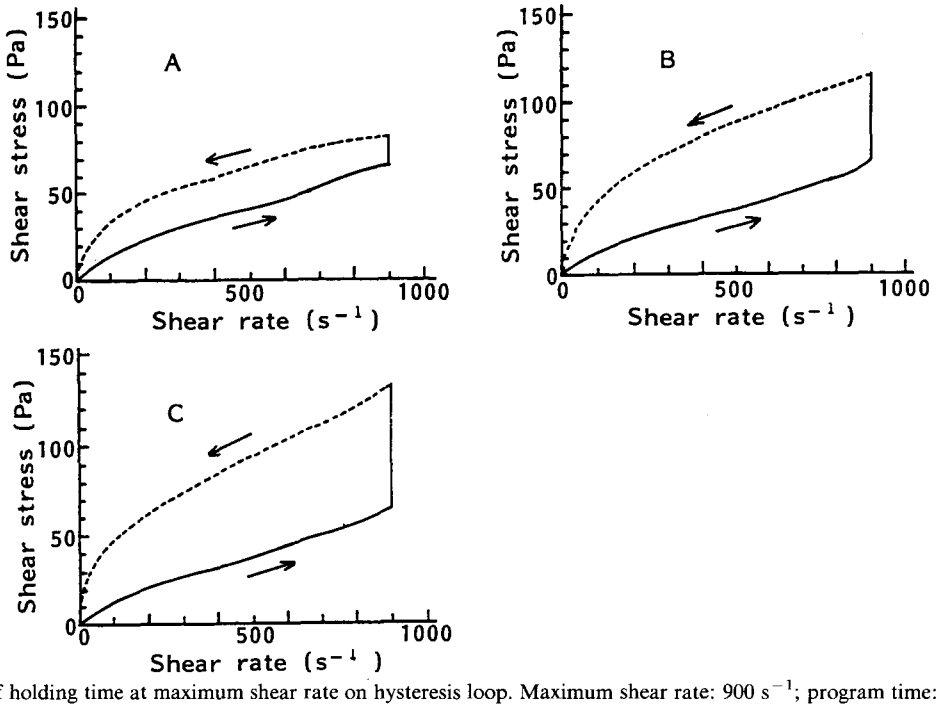

Fig. 6. Effect of holding time at maximum shear rate on hysteresis loop. Maximum shear rate: 900 s^{-1}; program time: 120 s. Holding time at maximum shear rate: (A) 60 s, (B) 120 s, (C) 180 s.

was indicated by the increase in k of the descending curves.

In conclusion, the negative thixotropy and viscosity of the w/o/w emulsion increased with increasing shear on increasing shearing time, repeating times of shear, and accelerating the rotation speed of the cone as shown in Tables 1 and 2.

Shear-induced phase-inversion of w/o/w emulsion with high shear

Fig. 7 shows flow curves of the w/o/w emulsion under uniform acceleration of rotation of the cone over a wider range of shear rate ($\dot{\gamma} > 200$ s^{-1}). In Fig. 7, $\dot{\omega}$ shows angular acceleration of the cone rotation.

TABLE 2

Parameters in Eqn 13 and loop areas of flow curves affected by maximum shear rate, repeating shear and holding time

Maximum shear rate (s^{-1})	Program time (s)	Repeating number	Holding time at maximum shear (s)	Ascending curve			Descending curve			Loop area (Pa s^{-1})
				a	k	r [a]	a	k	r [a]	
180	60	1	0	0.579	0.663	0.9982	0.594	0.614	0.9985	53.3
360	120	1	0	0.582	0.695	0.9983	0.572	0.748	0.9994	86.0
900	300	1	0	0.576	0.234	0.9956	0.490	1.592	0.9953	6370.2
900	120	1	0	0.580	0.833	0.9993	0.653	0.553	0.9822	961.2
900	120	2	0	0.566	0.958	0.9985	0.459	2.183	0.9964	4849.2
900	120	3	0	0.589	1.084	0.9927	0.435	3.518	0.9973	8607.6
900	120	1	60	0.659	0.680	0.9953	0.415	4.948	0.9976	19960.2
900	120	1	120	0.728	0.424	0.9977	0.450	5.376	0.9963	39688.8
900	120	1	180	0.720	0.450	0.9974	0.443	6.160	0.9924	46323.0

[a] r: correlation coefficient.

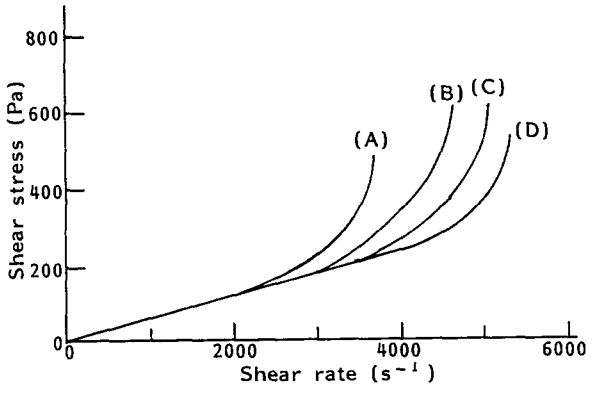

Fig. 7. Changes in flow curves on acceleration of shear rate. $\dot{\omega}$: (A) 0.17 rad/s^2, (B) 0.26 rad/s^2, (C) 0.35 rad/s^2, (D) 0.44 rad/s^2.

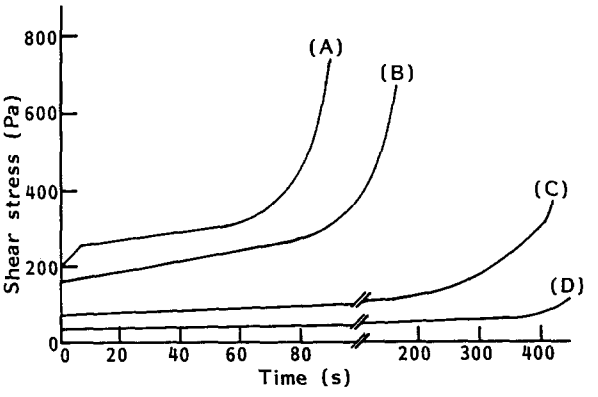

Fig. 8. Changes in flow curves with shear rate. Shear rate: (A) 5400 s^{-1}, (B) 3600 s^{-1}, (C) 1800 s^{-1}, (D) 900 s^{-1}.

Each curve has a critical point, where shear stress rapidly increased. The emulsions more sheared than the critical point became semi-solid. This semi-solid emulsion was hardly dispersed into water, but easily dispersed into chloroform.

The w/o/w emulsion containing sodium chloride and glucose in the inner and outer aqueous phases, respectively, was sheared and the changes in degree of entrapment of the markers were investigated. The percentages entrapped were calculated using Eqns 8 and 9 as shown in Table 3. The maximum shear rate and program time were 5400 s^{-1} and 120 s, respectively.

The percentages of entrapped markers in sheared emulsion increased markedly compared to those of the original w/o/w emulsion; 91.1% of glucose added to the outer aqueous phase during the preparation of the w/o/w emulsion became entrapped in the inner phase of the sheared emulsion. This sheared emulsion was semi-solid and readily dispersed into chloroform. Those findings suggested that the phase inversion from the w/o/w to w/o type emulsion occurred by intensive shearing.

Fig. 8 shows the changes in shear stress vs shearing time for various shear rates (900–5400 s^{-1}). These curves have critical points where shear stress rapidly increased, and the sheared emulsions changed to semi-solid w/o emulsions.

Umeya (1970) represented the relationship between shear stress (σ) of thixotropic fluid and shearing time (t) under constant shear rate by Eqn 15 derived by modifying Weltmann's empirical equation (Weltmann, 1943).

$$\ln \sigma = A - Bt \tag{15}$$

TABLE 3

Changes in percentages of water-soluble markers trapped in inner aqueous phase before and after shearing w/o/w emulsion by cone-and-plate viscometer

Emulsion	P_{NaCl} (%)	$P_{glucose}$ (%)
Prepared w/o/w emulsion	74.4	13.6
Sheared emulsion	86.4	91.1

Maximum shear rate, 5400 s^{-1}; program time; 120 s.

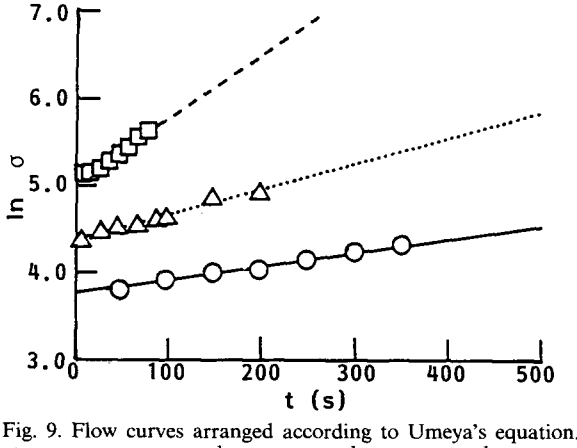

Fig. 9. Flow curves arranged according to Umeya's equation. Shear rate: (○) 900 s^{-1}, (△) 1800 s^{-1}, (□) 3600 s^{-1}. Correlation coefficient: (○) 0.9955, (△) 0.9961, (□) 0.9862.

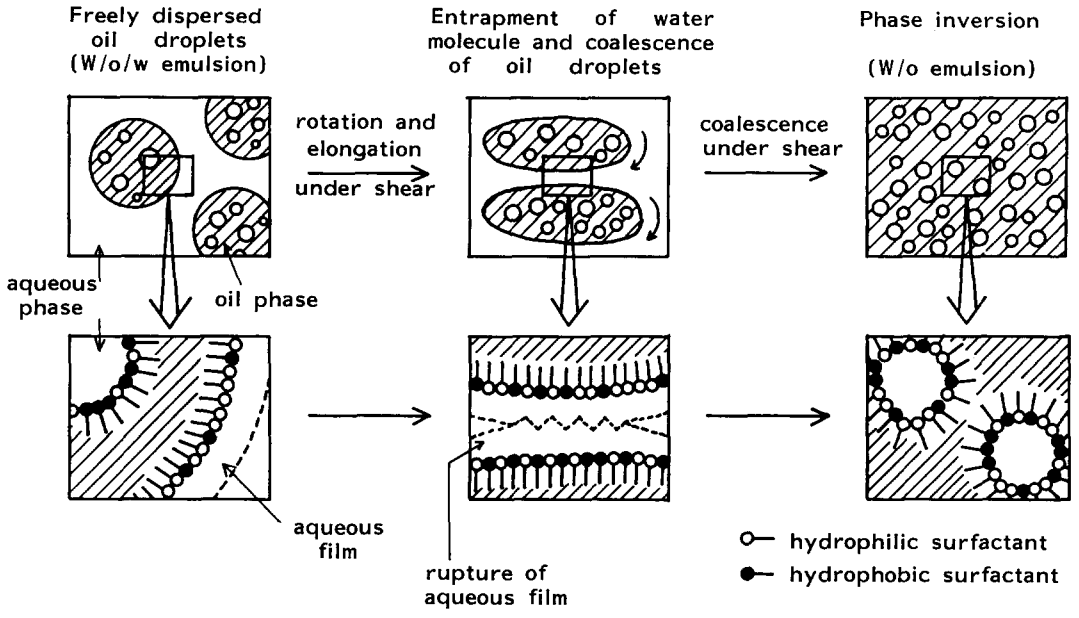

Fig. 10. Mechanism of phase-inversion under shear.

where A and B are constants. The relationship between $\ln \sigma$ vs t of the data in Fig. 8 up to the critical points is shown in Fig. 9. The good linearity in Fig. 9 indicates that thixotropic flow of sheared w/o/w emulsion occurred before phase inversion.

Discussion

The mechanisms of negative thixotropic flow and phase inversion to semi-solidified w/o emulsion

The negative thixotropy and increasing viscosities of w/o/w emulsions were observed by shearing under various conditions, e.g., prolonging cone rotation or repeating the shearing operation (Figs 2–6 and Tables 1 and 2).

It was assumed that the negative thixotropy at low shear resulted from an increase in the volume fraction of the oil droplets (dispersion phase) caused by shear-induced entrapment of water molecules in the oil droplets from the outer aqueous phase as shown in Table 3. Oil droplets might rotate and elongate on moving under shear. At the point of contact or in the region of two droplets, shear velocity should increase resulting in thinning of the aqueous film at the interface. A local thinning of the liquid film might lead to rupture of the film. The concentration of surfactant at the interface would become greater, where water molecules of ruptured film can be enclosed by surplus surfactant molecules. The surfactant molecules involving water molecules might migrate into oil droplets because of the deficiency of surfactant in the oil droplets.

Mooney (1951) represented the relative viscosity of emulsion (η_r) as follows,

$$\eta_r = \exp\{2.5\phi/(1 - k\phi)\} \tag{16}$$

where ϕ is the volume fraction of dispersion phase and k is a constant.

The negative thixotropy of the w/o/w emulsion might be explained by the increase in viscosity of the emulsion due to increase in ϕ in Eqn 16. At the same time, the oil droplet might coalesce because of the rupture of the aqueous film at the interface and the entrapment of water by surfactant molecules. When all the oil droplets have coalesced, phase inversion to w/o emulsion occurs

TABLE 4

Dissipation energy, kinetic energy and impulse applied for phase transition of w/o/w emulsion under uniform rotation shear

$\dot{\gamma}$ (s^{-1})	ω (rad/s)	t_c (s)	E_d ($\times 10^8$) (erg/cm^3)	E_k (cm^2/s^2)	M (dyn s)
900	5.24	385	1.55	58.2	8.99
1800	10.47	170	2.15	237.4	8.01
3600	20.94	85	4.88	940.4	7.98
5400	31.42	60	8.09	2122.8	8.46

under intensive shearing. The proposed mechanism of shear-induced phase inversion is illustrated in Fig. 10.

The volume fraction of the dispersed phase of the original w/o/w emulsion was 0.5 and that of the phase-inverted emulsion was about 0.81, calculated based on the formulation. Therefore, the phase-inverted w/o emulsion revealed markedly increased viscosity, i.e. semi-solid state.

Hydrodynamic parameter determining shear-induced phase inversion of w/o/w emulsion

Phase inversion occurred on shearing the w/o/w emulsion at critical points of the shear rate attained by uniformly accelerating the rotation of the cone (Fig. 7) or the shearing time at a constant shear rate (Fig. 8). Hydrodynamic parameters correlating to the critical point were found as follows. Assumed hydrodynamic parameters were the fluid energy (E_d) dissipated by the emulsion, impulse applied by the rotating cone to the emulsion (M) and kinetic energy (E_k) on phase inversion.

The dissipated energy per unit volume of fluid and time at which the flow of liquid has a velocity of η, $\dot{E}_d$, which is the differential amount of E_d with time, is represented as follows (Casson, 1959);

$$\dot{E}_d = \eta\dot{\gamma}^2 = \eta\omega^2/\Theta^2. \tag{17}$$

When the shearing time required to cause phase inversion is defined as t_c, E_d is represented by Eqn 18 at a constant rotation of cone or by Eqn 19 at uniform acceleration of rotation of the cone,

$$E_d = \int_0^{t_c} \dot{E}_d \, dt = \int_0^{t_c} \eta\omega^2/\Theta^2 \, dt = \eta\omega^2 t_c/\Theta^2 \tag{18}$$

$$E_d = \int_0^{t_c} \dot{E}_d \, dt = \int_0^{t_c} \eta(\dot{\omega}t)^2/\Theta^2 \, dt = \eta\dot{\omega}^2 t_c^3/3\Theta^2. \tag{19}$$

The kinetic energy per unit weight of fluid (E_k) is represented as follows (Appendix):

$$E_k = \omega^2 R^2/10, \tag{20}$$

where R is the radius of the cone.

The force due to the viscosity of emulsion under rotational shear is calculated as follows;

$$F = \int_0^R \eta\dot{\gamma} \times 2\pi r \, dr = \pi\eta R^2/\Theta, \tag{21}$$

where r is the distance from the center of the plate to an arbitrary point in the liquid placed between the cone and plate. The impulse applied to the emulsion by rotating the cone until inducing phase inversion (M) is calculated as follows for a constant shear rate;

$$M = \int_0^{t_c} \pi\eta\omega R^2/\Theta \, dt = \pi\eta\omega R^2 t_c/\Theta \tag{22}$$

TABLE 5

Dissipation energy, kinetic energy and impulse applied for phase transition of w/o/w emulsion under uniformly accelerated rotation shear

$\dot{\omega}$ (rad/s^2)	ω_c (rad/s)	t_c (s)	E_d ($\times 10^8$) (erg/cm^3)	E_k (cm^2/s^2)	M (dyn s)
0.17	20.4	115	2.71	896.0	5.50
0.26	25.0	96	3.68	1345.6	5.38
0.35	29.8	85	4.63	1912.0	5.68
0.44	33.9	77	5.44	2474.2	5.86

and

$$M = \int_0^{t_c} \pi\eta\omega R^2/\Theta \, dt = \int_0^{t_c} \pi\eta\dot{\omega}tR^2/\Theta \, dt$$

$$= \pi\eta\dot{\omega}R^2 t_c/2\Theta \qquad (23)$$

for uniformly accelerated rotation of the cone.

Tables 4 and 5 show the values of E_d, E_k, and M calculated by using Eqns 18–20, 22 and 23. ω_c in Table 4 and 5 represents the angular velocity at the phase inversion of the emulsion.

E_d and E_k varied, increasing with increase in $\dot{\gamma}$ or $\dot{\omega}$. However, M remained almost constant under constant rotation or uniformly accelerated rotation of the cone, suggesting that M was a parameter determining the phase inversion. M under constant rotation was greater than that under uniformly accelerated rotation. This difference might be caused by slipping of the cone at the start of rotation with constant speed.

In the present study, it was found that shear-induced phase inversion of the w/o/w emulsion occurred when an impulse stronger than the critical value given in Tables 4 and 5 was applied to the emulsion by the cone.

Further viscoelastic investigations, i.e., creep test and oscillation test etc., suggested by Barry (1973, 1974), Kirikou (1979) and Kobayashi et al. (1982), should be performed in order to characterize more precisely the rheological properties of the present w/o/w emulsion.

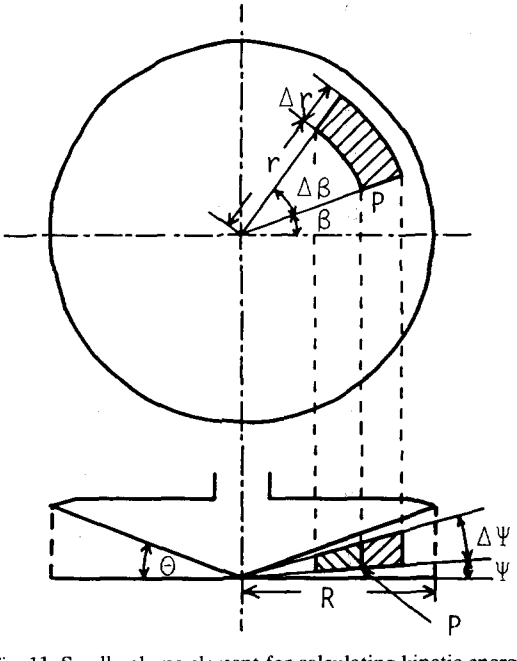

Fig. 11. Small volume element for calculating kinetic energy.

Appendix

Calculation of the kinetic energy of flowing emulsion (Eqn 20)

Assuming the hatched volume element in Fig. 11. The origin was placed at the center of the plate of the viscometer. The position vector, $\vec{p}$ of P, the edge point of the volume fraction, and ΔV, the hatched volume, are calculated as follows, respectively:

$$\vec{p} = (r\cos\beta,\ r\sin\beta,\ r\tan\psi) \qquad (A1)$$

$$\Delta V = \int_r^{r+\Delta r}\int_\beta^{\beta+\Delta\beta}\int_\psi^{\psi+\Delta\psi} |(\partial\vec{p}/\partial\beta)$$

$$\times(\partial\vec{p}/\partial\psi)|\,d\psi\ d\beta\ dr$$

$$= r^2\,\Delta\beta\,\Delta r\{\tan(\psi+\Delta\psi) - \tan\psi\}. \qquad (A2)$$

$$\lim_{\Delta\psi\to 0}\{\tan(\psi+\Delta\psi) - \tan\psi\}/(\sec^2\psi\,\Delta\psi) = 1 \qquad (A3)$$

Eqn A2 is simplified as follows by substituting Eqn A3,

$$\Delta V = r^2\sec^2\psi\,\Delta\beta\,\Delta r\,\Delta\psi \qquad (A4)$$

The velocity, v_p at position, P is,

$$v_p = r\omega\tan\psi/\tan\Theta. \qquad (A5)$$

The kinetic energy of flow of the w/o/w emul-

sion in the volume element, ΔE_k is represented as follows;

$$\Delta E_k = \rho \Delta V v_p^2/2 = \{\rho r^4 \omega^2 (\tan^2 \psi/\tan^2 \Theta) \times \sec^2 \psi/2\} \Delta\psi \, \Delta\beta \, \Delta r, \quad \text{(A6)}$$

where ρ is the density of the w/o/w emulsion.

The total kinetic energy of the emulsion between the cone and plate of the viscometer (W) is

$$W = \int_0^R \int_0^{2\pi} \int_0^{\Theta} \{\rho r^4 \omega^2 (\tan^2 \psi/\tan^2 \Theta) \times \sec^2 \psi/2\} \, d\psi \, d\beta \, dr$$

$$= \rho \omega^2 \pi R^5 \tan \Theta/15. \quad \text{(A7)}$$

The volume of emulsion between cone and plate (V) is

$$V = \int_0^R \int_0^{2\pi} \int_0^{\Theta} r^2 \sec^2 \psi \, d\psi \, d\beta \, dr$$

$$= 2\pi R^3 \tan \Theta/3. \quad \text{(A8)}$$

The kinetic energy per unit mass of the emulsion (E_k) is calculated as follows;

$$E_k = W/\rho V = \omega^2 R^2/10. \quad \text{(A9)}$$

Acknowledgments

The taking of electron micrographs of the w/o/w emulsion by Mr Toshiaki Suzuki (JEOL, Ltd) is much appreciated.

References

Barry, B.W., Rheology of pharmaceutical and cosmetic semi-solids. *Adv. Pharm. Sci.*, 4 (1974) 1–72.

Barry, B.W. and Eccleston, G.M., Oscillatory testing of o/w emulsions containing mixed emulsifiers of the surfactant-long chain alcohol type: self-bodying action. *J. Pharm. Pharmacol.*, 25 (1973) 244–253.

Casson, N., A flow equation for pigment-oil suspensions of the printing ink type. In Mill, C.C. (Ed.), *Rheology of Disperse Systems*, Pergamon, London, 1959, pp. 84–104.

Dubois, M., Gilles, K.A., Hamilton, J.K., Rebers, P.A. and Smith, F., Calorimetric method for determination of sugars and related substances. *Anal. Chem.*, 28 (1956) 350–356.

Fukushima, S., Juni, K. and Nakano, M., Preparation of and drug release from w/o/w type double emulsions containing anticancer agents. *Chem. Pharm. Bull.*, 31 (1983) 4048–4056.

Garti, N., Magdassi, S. and Whitehill, D., Transfer phenomena across the oil phase in water-oil-water multiple emulsions evaluated by Coulter Counter. 1. Effect of emulsified 1 on water permeability. *J. Colloid Interface Sci.*, 104 (1985) 587–591.

Kirikou, M. and Sherman, P., The influence of Tween 40/Span 80 ratio on the viscoelastic properties of concentrated oil - water emulsions. *J. Colloid Interface Sci.*, 71 (1979) 51–54.

Kobayashi, M., Ishikawa, S. and Samejima, M., Application of nonlinear viscoelastic analysis by the oscillation method to some pharmaceutical ointments in the Japanese Pharmacopeia. *Chem. Pharm. Bull.*, 30 (1982) 4468–4478.

Lin, T.J., Kurihara, H. and Ohta, H., Effects of phase inversion and surfactant location on the formation of o/w emulsions. *J. Soc. Cosm. Chem.*, 26 (1975) 121–139.

Magdassi, S. and Garti, N., A kinetic model for release of electrolytes from w/o/w multiple emulsions. *J. Controlled Release* 3, (1986) 273–277.

Matsumoto, S., Kita, Y. and Yonezawa, D., An attempt at preparing water-in-oil-in-water multiple-phase emulsions. *J. Colloid Interface Sci.*, 57 (1976) 353–361.

Matsumoto, S., Inoue, T., Kohda, M. and Ikura, K., Water permeability of oil layer in w/o/w emulsions under osmotic pressure gradients. *J. Colloid Interface Sci.*, 77 (1980) 555–563.

Matsumoto, T., Takashima, A., Masuda, T. and Onogi, S., A modified Casson equation for dispersions. *Trans. Soc. Rheol.*, 14 (1970) 617–620.

Mooney, M., The viscosity of a concentrated suspension of spherical particles. *J. Colloid Sci.*, 6 (1951) 162–170.

Ohmotosho, J.A., Whateley, T.L., Law, T.K. and Florence, A.T., The nature of the oil phase and the release of solutes from multiple (w/o/w) emulsions. *J. Pharm. Pharmacol.*, 38 (1986) 865–870.

Takahashi, Y., Applications of w/o/w type multiple phase emulsions to dairy product substitutes. *J. Jap. Oil Chem. Soc.*, 35 (1986) 880–888.

Umeya, K., Isoda, T. and Koizumi, G., Thixotrophy, *J. Materials Sci. Soc. Jap.*, 7 (1970) 134–143.

Weltman, R.N., Breakdown of thixotropic structure as function of time. *J. Appl. Phys.*, 14 (1943) 343–350.

Yoshioka, T., Ikeuchi, K., Hashida, M., Muranishi, S. and Sezaki, H., Prolonged release of bleomycin from parenteral gelatin sphere-in-oil-in-water multiple emulsion. *Chem. Pharm. Bull.*, 30 (1982) 1408–1415.